

## ACTIVE CONTROL ISSUES FOR THE CALIFORNIA EXTREMELY LARGE TELESCOPE

D. G. MacMartin\*  
California Institute of  
Technology

G. Chanan‡  
University of California,  
Irvine

T. S. Mast†  
University of California,  
Santa Cruz

J. E. Nelson§  
University of California,  
Santa Cruz

### Abstract

A team of researchers from the University of California and Caltech are investigating the feasibility of building a 30 meter diameter segmented mirror telescope, following the design approach pioneered by the 36-segment Keck telescopes. The current design concept for the California Extremely Large Telescope (CELT) has 1080 segments forming the primary mirror, with the piston, tip, and tilt of each segment controlled by three actuators. The control approach must correct for gravity- and temperature-induced deformations of the mirror support structure, and potentially wind and seismic disturbances, with a cost effective design. We discuss some of the active control issues, including requirements (optical and cost), estimates of the disturbances, actuator options, and control analysis. Several candidate actuator technologies appear capable of meeting the technical and cost requirements, and preliminary error propagation analyses indicate that the optical error budget can likely be met. Additional issues being addressed are identified.

### 1. Introduction

The largest optical and infrared telescopes in the world today are the Keck telescopes on Mauna Kea in Hawaii, the first of which became operational in 1992. Each telescope's 10 meter diameter primary mirror is a mosaic of 36 hexagonal segments, with three actuators on each segment and two capacitive sensors on each inter-segment edge. Conceptual design work is now underway on a 30 meter diameter telescope<sup>1</sup>, shown in Figure 1. This telescope would have 9 times the collecting area of each Keck telescope, and with adaptive optics to correct for atmospheric distortion, could achieve diffraction-limited angular resolution of 0.007 arcseconds at a wavelength of 1 $\mu$ m. Using a traditional scaling of  $D^{2.5}$  for telescope construction

cost with size suggests that cost will be a very significant factor in design decisions<sup>2</sup>. The current conceptual design phase will therefore assess the technical and cost feasibility. Initial efforts include the active control of the primary mirror discussed herein.

At Keck, the in-plane motion of each segment of the primary mirror is passively constrained, while the three out of plane degrees of freedom are actively controlled. This requires a total of 108 actuators, compensating for gravity and thermal deformations by feeding back information from 168 edge sensors at a 2 Hz update rate<sup>3,4</sup>. The initial design concept for CELT has 1080 hexagonal segments, 3240 actuators, and 6204 edge sensors<sup>1</sup>. In addition to increasing the overall size of the telescope relative to Keck, the size of each segment has decreased. This allows thinner segments to be used, which in turn reduces the weight of the primary mirror (which impacts numerous other subsystems), material costs, and polishing costs. However, as a result, CELT has 30 times the number of segments, and therefore 30 times the number of actuators. Each segment of the primary mirror will have three displacement actuators, as in Keck, and each inter-segment edge will have two capacitive sensors that measure the relative displacement between neighboring segments, as illustrated schematically in Figure 2. Wavefront information is also likely to be used to estimate the lowest wave-number distortions of the primary mirror. Reference 1 describes the current design concept for the overall telescope. The segment geometry is illustrated in Figures 5 and 6. References 5 and 6 describe the preliminary design concepts for the active control hardware, and preliminary control analysis, respectively.

---

Copyright © 2001 by the authors. Published by the American Institute for Aeronautics and Astronautics with permission.

\* Dept. of Control and Dynamical Systems, MS 104-44, Pasadena, CA, 91125, [macmardg@cds.caltech.edu](mailto:macmardg@cds.caltech.edu).

Senior Member AIAA.

† Dept. of Astronomy and Astrophysics, Santa Cruz, CA 95064, [mast@ucolick.org](mailto:mast@ucolick.org)

‡ Dept. of Physics and Astronomy, Irvine CA 92627, [gchanan@galaxy.ps.uci.edu](mailto:gchanan@galaxy.ps.uci.edu)

§ Dept. of Astronomy and Astrophysics, Santa Cruz, CA 95064, [jnelson@ucolick.org](mailto:jnelson@ucolick.org)

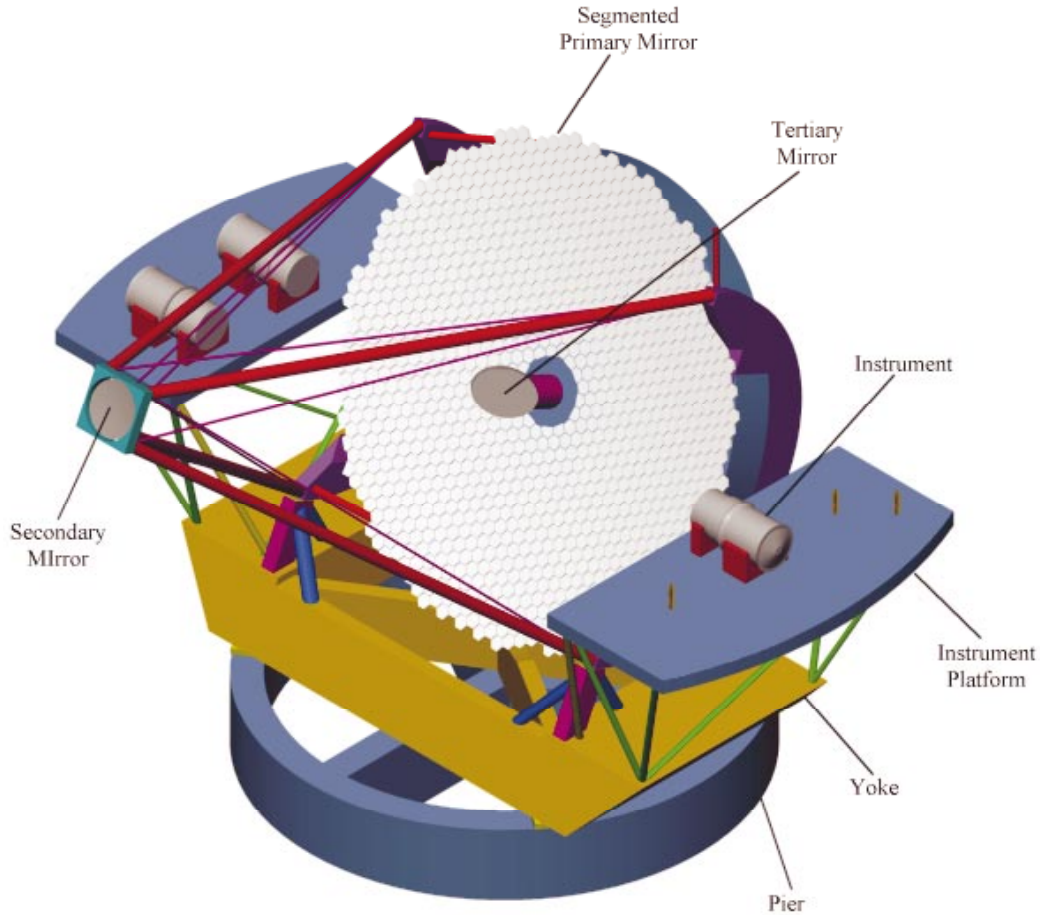


Figure 1. Artist's conception of the California Extremely Large Telescope (CELT).

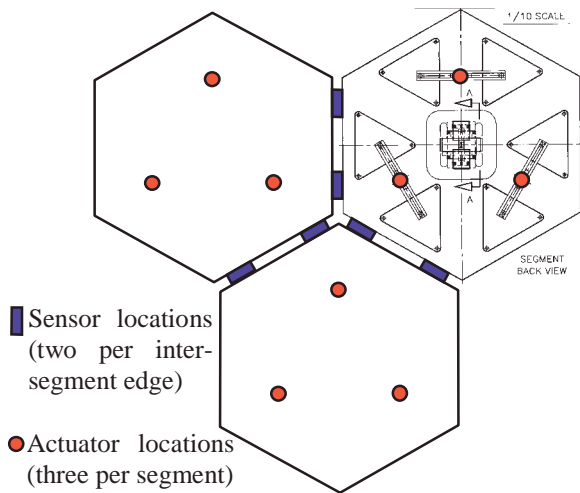
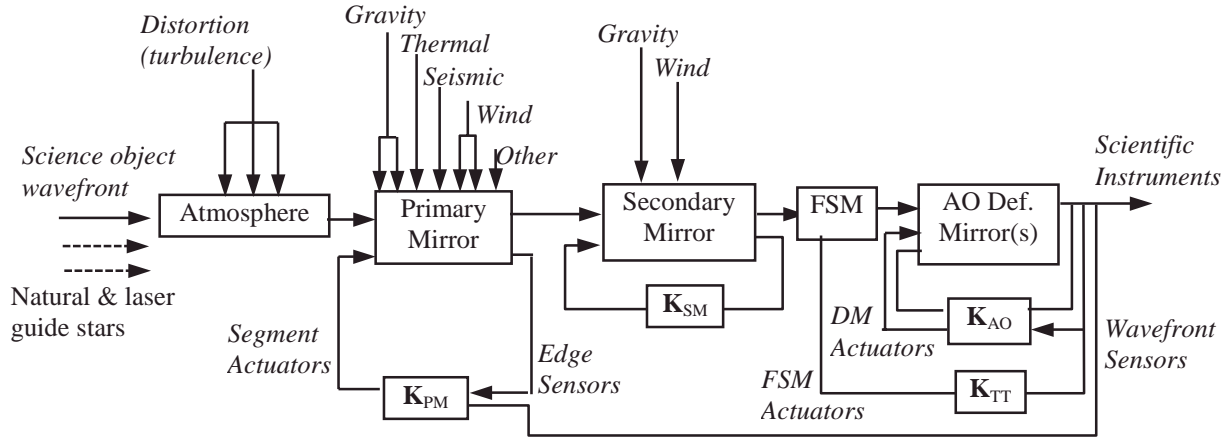


Figure 2. Schematic of sensor and actuator arrangement on mirror segments. The upper right segment shows the distribution of forces over the mirror through the whiffle tree.

The surface of the primary mirror must maintain the desired shape with an accuracy of a small fraction of a wavelength. The overall control problem is represented in Figure 3. The primary mirror is affected by gravity (directly, and indirectly through deformations of the main journals), thermal variations (both overall temperature and thermal gradients), wind disturbances (directly on the primary and secondary support structures, and possibly on the dome), and vibrations from various drives and motors or seismic activity. To control the resulting wavefront distortion, the primary mirror will have an active optics system including displacement actuators, edge sensors, and potentially wavefront information. The position of the secondary mirror is also influenced by both gravity and wind, and therefore active control will likely also be required for low bandwidth positioning of the secondary. In addition to these control loops, an adaptive optics (AO) system will be available to compensate for turbulence-induced distortion of the wavefront as it propagates through the atmosphere. The AO system will also correct for the low-frequency component of the above perturbations in the primary mirror.



**Figure 3. Block diagram for CELT wavefront propagation, left to right. Disturbances are shown at the top of the figure, and possible control loops at the bottom. The primary mirror is affected by gravity, thermal, seismic, wind, and other disturbance sources. Control of the primary mirror uses feedback from both edge sensors and possibly wavefront sensors. Additional control loops are needed for positioning of the secondary mirror, and for the adaptive optics (AO).**

This paper provides an overview of some of the issues associated with the active control of the primary mirror for CELT. The optical requirements that the control system must meet are defined next, followed by the current estimate of the disturbances that the active control system needs to correct. Preliminary feasibility analysis can be separated into two aspects. First, we present a preliminary assessment of hardware options for actuation and sensing, to meet both technical (precision, stroke) and implementation (cost, reliability) goals. Second, we present control analyses to assess the ability to meet the required wavefront specification in the presence of the disturbances; these analyses focus on the resulting precision, but must also address bandwidth and computational requirements. The problems are clearly challenging. At this stage, the technical and cost issues for the active control system appear to be feasible. Issues requiring further work will be discussed in the summary.

## 2. Requirements

CELT will operate in two modes, seeing limited (adaptive optics off), and diffraction limited (adaptive optics on), with different error budgets. With adaptive optics off, the goal is to degrade atmospheric seeing by less than 10%, yielding a requirement on the telescope to provide  $\theta(80) \leq 0.26$  arc seconds, where  $\theta(80)$  is the 80% enclosed energy diameter measured in arcseconds on the sky. This overall error must allow for errors in the primary, secondary, and tertiary mirrors, plus guiding errors. Several factors contribute to the primary mirror surface, including polishing errors (figuring), gravity and thermal deflections within a segment, in-plane segment motion, and the actively controlled out-of-plane motion. The current error budget for AO off therefore allocates  $\theta(80)=0.066$

arcseconds for control errors, including the error in desired sensor readings, sensor noise, actuator noise, and residual vibration above the control bandwidth.

The error budget with AO on is similarly intended to ensure that the telescope does not dominate the wavefront quality, measured in nanometers. The current requirement is no more than 50 nm rms of uncorrectable wavefront error due to the primary mirror. Low wavenumber distortions of the primary mirror can be corrected by the adaptive optics system (provided that this does not result in saturation of the AO actuators), so this error budget applies primarily to high wavenumber errors such as edge discontinuities. The error budget for active control errors is 22.3 nm, leading to a requirement that the impact of sensor noise, actuator noise, and uncontrolled frequencies each need to be in the 10-15 nm range.

The active control system must also meet “reasonable” cost and reliability requirements. The system cost and reliability will be determined primarily by the unit cost and reliability of the actuators and sensors. Since a single actuator failure would result in inability to meet performance, failures should be kept to one or two per year at most. Sensor failures can be tolerated, since the control problem is substantially over-determined (6204 sensors for 3240 degrees of freedom). The cost target per actuator is \$2000, including all electronics, local sensing, and cabling; although aggressive, this target will still result in over \$6M for the actuators alone.

## 3. Disturbances

The design and analysis of the control system requires estimates of the disturbances on the primary mirror. Disturbance sources include gravity deformations,

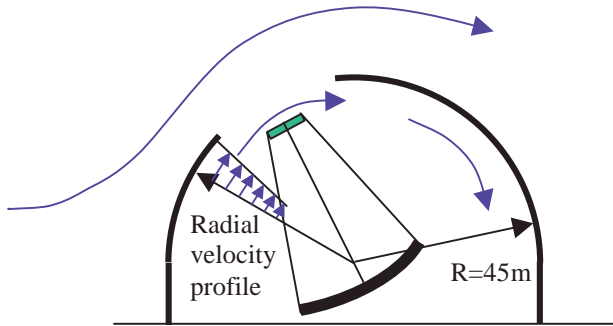


**Figure 4. Schematic of telescope dome exposed to wind, and resulting internal wind pattern.**

thermal variations, wind, and vibrations from drives and motors.

First, we briefly describe the support structure for the primary mirror. The in-plane degrees of freedom of each segment are passively supported, while piston, tip, and tilt are actively controlled. Each of the three actuators connects to the segment through a whiffletree that distributes the load over six points, for a total of 18 support points (shown in Figure 2). The resonance of a segment on the whiffletree is currently estimated to be ~60 Hz (compared with ~30 Hz for Keck). The mirror cell that supports the entire primary mirror is a lightweight space frame. The mirror cell compliance only results in significant deflection for disturbances such as gravity that are correlated across many segments. For forces (e.g. wind) that are uncorrelated over distances of a few segments, the net deflection due to the mirror cell compliance is small, and the total deflection is dominated by the whiffletree compliance.

Gravity is the largest amplitude disturbance source, and therefore drives the actuator stroke requirement. As the elevation angle of the telescope changes, the changing direction of gravity deforms the mirror cell, resulting in a parabolic sagging of the cell. The current estimate is that a stroke of ~1.2 mm is required for each actuator to compensate for the difference in deflection between inner and outer segments. Since the changes in gravity due to orientation occur only slowly, this disturbance source does not require high control bandwidth. During observations, the 1.2 mm total deflection will occur as the telescope tracks from horizon to zenith in 6 hours, with a maximum variation of roughly 70 nm/s. Thermal variations also will be slow, and smaller in magnitude (on the order of 10  $\mu$ m). Therefore, any control system that can mitigate the gravity disturbance can also mitigate thermal effects, and hence these disturbances do not impact the control requirements.

Wind disturbances on the Keck telescopes are of insufficient amplitude to require control, however, this

may not be true for the larger CELT telescope. If the wind disturbance amplitude is sufficient to require some active control, its spectrum will drive the requirements on the control system bandwidth and actuator slew rate. Wind must also be accounted for in the design of the secondary mirror support system.

The primary resource used to estimate wind-induced deflections of the CELT primary mirror is data collected at Gemini South<sup>7</sup>, one of a pair of 8m telescopes. Additional information is available from a wind tunnel test performed during the design of Keck<sup>8</sup>, and computational modeling for Gemini<sup>9</sup>. The Gemini data includes wind speed measurements external to the dome, at the secondary mirror, and at three locations on the primary mirror, as well as 24 pressure measurements distributed across the primary. The Gemini telescopes have large vents that can open to flush the dome, and we have only used data taken with these closed in extrapolating to CELT.

Although the site for CELT has not yet been determined, Mauna Kea is a candidate. Wind speeds at the summit exceed 14 m/s 5% of the time<sup>10</sup>. To ensure telescope operability in most conditions, this speed will be assumed for this analysis. Wind speeds within the dome vary with the orientation of the telescope relative to the wind. The worst-case orientation is with the dome opening pointing into the wind, and for elevation angles mid-way between horizon and zenith, as shown in Figure 4. At these orientations, the wind passing over the dome opening tends to set the air within the enclosure into rotation<sup>8</sup>. The data collected at Gemini indicates a worst-case wind speed at the secondary of about 35% of the external wind speed. The wind tunnel tests and Gemini modeling gave a slightly lower estimate. For the worst-case orientations, the wind speed over the Gemini primary mirror is about 7% of the external wind speed. Since the ratio of dome opening to diameter for CELT is likely to be about 30% higher than for Gemini (32.5 m/90 m instead of 10 m/36 m), we will assume that the internal wind speeds are similarly increased. Thus for the purposes of analysis, we will assume the rms wind at the primary mirror will not exceed 10% of the external speed.

The Gemini data also confirm the correspondence between the spatial rms of the measured pressure, and the dynamic pressure computed from the wind speed. Thus an estimate of the wind loading on each segment can be obtained from the dynamic pressure and the segment area  $A_s = 0.65 \text{ m}^2$  (hexagon 0.5 m on a side). For Mauna Kea, the air density is  $\rho = 0.8 \text{ kg/m}^3$ , thus

$$F = \frac{1}{2} \rho V_p^2 A_s$$

yields an rms force of 0.5 N per segment.

To estimate the segment deflection due to this estimated wind force requires a structural model, the force distribution, and the spatial coherence of the forces. At this point in the preliminary design of CELT, such a structural model is unavailable. The spatial coherence of the pressure can be estimated, again from Gemini data, as decreasing roughly linearly to zero at 3-5 m. Thus the deflections will be dominated by the contribution from the whiffletree compliance, leading to roughly 50 nm rms deflection due to the 0.5 N rms force per segment. Using the worst-case coherence estimate, the approximate moment can also be estimated, and hence the segment tip and tilt. The resulting rms segment rotation is  $\sim 3$  milli-arcseconds, yielding a contribution to  $\theta(80)$  of  $\sim 3.6$  mas. The resulting edge discontinuities from differential piston between segments is 40 nm rms. For an AO system with  $\sim 2.5$  actuators across a segment, this leads to an uncorrectable wavefront error of  $\sim 15$  nm rms.

Since the static load due to the wind can be controlled by the active control system, we also need the spectrum of the dynamic response to assess the energy above the control system bandwidth. There are two dynamic sources; the inherent variation in the original external wind speed, and turbulence caused by the interaction of a steady wind on the structure. Gemini wind spectra show a  $f^{-2/3}$  roll-off rate consistent with Kolmogorov turbulence, with a corner frequency of  $\sim 0.03$  Hz. The overall form of the pressure spectrum is less clear but appears to have a similar roll-off rate and a higher corner frequency. Roughly  $1/3$  of the energy is above 0.1 Hz, and only about 10% is above 1 Hz. The response due to the wind of the 60 Hz resonance of the segment / whiffletree dynamics can be estimated from the spectrum, the amplification of the resonance (assume  $Q \approx 50$ ) and the equivalent bandwidth  $(\pi/2)(2\pi f_0)Q^{-1}$  of the resonator. The result is highly dependent on the assumed high frequency pressure spectrum, but could add significant energy.

The wind-induced primary mirror response for Keck was predicted to be 44 nm rms<sup>11</sup>. While the Keck worst-case wind vibration did not exceed the error budget allocated to it, the worst-case wind vibration of the primary mirror for CELT may require attention. The estimates presented here are highly dependent on the assumptions made for the reduction in wind speed within the telescope enclosure, the spatial correlation of the resulting pressure, and the spectrum. Further analysis will be conducted in the preliminary design phase. If the wind remains an issue when more accurate analyses are conducted, then either the bandwidth of the active control system must be increased, or passive means used such as wind fences outside the dome opening.

Our current estimate of disturbances, then, includes two primary sources that influence the control design. Low frequency, large amplitude gravity deflections define the total stroke required. The possibility that wind-induced vibration will require control raises the possibility that a control bandwidth higher than that used on the Keck telescopes may be required. The feasibility of meeting the optical and cost requirements in the presence of these disturbances can be considered in two parts: the control hardware (actuation and sensing), and the analysis of precision and bandwidth.

#### 4. Actuators and control hardware

The Keck telescopes use a custom actuator design that includes a roller screw and a 24:1 hydraulic motion reducer<sup>12</sup>. These actuators cost roughly \$7000 each, and have an overall failure rate (for 108 actuators) of roughly one per year. Since CELT will have 30 times the number of actuators, this would result in a \$25M cost if the same design approach were followed, and an unacceptable overall reliability. Experience with Keck indicates that the roller screws themselves are quite reliable, while there are occasional problems with the hydraulic motion reducer.

For CELT, we are seeking more than a three-fold reduction in the unit cost of the actuators, while increasing the precision requirement, increasing the stroke, and increasing the reliability requirement. For reliability, the goal is that at the end of 10 years of operation, the probability of any given actuator failing will be less than 1 in 2000 per year. Table 1 compares a few of the key actuator requirements for Keck and for CELT. The cost goal listed in the table includes all electronics (including local sensor and servo loops) and cabling. There are also axial and transverse stiffness and load requirements. In addition, the actuator must operate in the temperature environment, have low power dissipation, be dust protected, and have easy installation and removal.

Various actuator technologies have been investigated, considering both the technical specifications and the development required<sup>13</sup>. Key challenges are cost, reliability, and simultaneously achieving excellent resolution with a (relatively) large stroke. The options considered fall into four categories:

- (i) roller or ball screw with some means for motion reduction,
- (ii) two-stage devices,
- (iii) inchworm devices, or
- (iv) direct actuation with smart materials.

It is likely that the requirements can be met or nearly met with either of the first two candidate approaches, therefore the other approaches are not currently being considered. Each approach is discussed below.

	<b>Keck</b>	<b>CELT</b>
Range	> 0.6 mm	> 1.2 mm
Rms position error	< 20 nm	< 7 nm
Slew rate	> 10 $\mu\text{m/s}$	> 10 $\mu\text{m/s}$
Axial load capacity	> 150 kg	> 30 kg
Reliability @ 10 yrs	< 1 in 30	< 1 in 2000
Cost	> \$7000 ea	< \$2000 ea

**Table 1. Comparison of Keck and CELT actuator specification.**

Ball or roller screws are attractive candidates since they are readily available commercially, reliable, and have no limitations (for this application) on achievable stroke. In either case, motion reduction is required to obtain the desired precision. Because of the cost issue on CELT, ball screws may be preferable due to their inherently lower cost. Typically, stiction and life issues are worse for ball screws, however, because of the smaller segment size, the actuators do not need to push against as large a load as with Keck (life typically varies as the load cubed). Rather than use a hydraulic reduction stage, an innovative mechanical reduction is being considered that will be easier to manufacture, cheaper, and more reliable. Design of a sensor for a servo loop is straightforward, since an interpolated encoder can be used, as was done for Keck<sup>12</sup>.

Two-stage devices, where a coarse stage provides the stroke and a precision stage the resolution, are attractive if each stage can, as a result, be made substantially cheaper. The large stroke actuator could be an inexpensive DC motor, for example. Sufficient precision can be obtained with either voice coil or solid state actuation such as piezoelectric or electrostrictive materials. A voice coil is likely to be cheaper and more reliable, although it adds the complication of a soft actuator where the stiffness must be obtained through closing a servo loop. There is a resulting slight increase in the high frequency wind loading on the primary mirror. However, with a stiff precision stage, care must be taken in the design and validation of the control algorithms to ensure that no short duration spike in the overall displacement of the device occurs each time the coarse stage device takes its minimum resolution step. A precision sensor is required for servo loop design; an inductive sensor appears to be available and reasonable in cost. Such a sensor did not exist during the Keck design phase, and thus these two-stage devices could not easily be designed. If a two-stage design is selected, it may, of course, be possible to physically separate the two stages; that is, to have the high stroke actuator acting on a group of segments, and precision control on each individual segment, as suggested in Ref. 5. However, this adds significant complication to the overall structural design of the mirror cell, and will

therefore be avoided unless shown to have a dramatic impact on the cost of the active control system.

Inchworm devices can effectively increase the stroke of a precision actuator. Several devices are commercially available (e.g. from Burleigh). However, since the holding power of the grip is through friction, the load capacity is too limited for our application. One design that overcomes this limitation uses MEMS fabrication to create mating ridges on each of the gripping surfaces<sup>14,15</sup>. Substantially higher axial loads can therefore be tolerated. It appears possible to design such a device that has sufficient stroke, force capability, and precision for CELT. However, further validation work would be required, and reliability and cost are uncertain.

While solid state materials (such as piezoelectric, electrostrictive, or magnetostrictive) have sufficient precision for this application, the stroke requirement eliminates them from consideration. The total stroke and force for CELT determine the energy the actuator must be able to produce. Any motion amplification will only increase the energy requirement due to losses<sup>16</sup>. A comparison with material energy density immediately gives the minimum amount of material, and hence the cost, which for this application becomes prohibitive. For example, with magnetostrictive material, each actuator would require ~5 kg of material, costing roughly \$5000, without including any of the housing or electronics for the actuator. Other innovative actuation technologies have also been considered, but do not currently appear to be as attractive as candidates from either of the first two approaches.

Two types of sensors will be used. Capacitive edge sensors, similar in concept to those used at Keck, measure relative displacement between neighboring segments<sup>5</sup>. The Keck sensors have a noise level as measured in operation at the telescope of roughly 6 nm. These sensors have precision components mounted in an interlocking "paddle" below the two segments<sup>17</sup>, resulting in a costly design, and complicated installation and maintenance. Because CELT requires more than 6000 such sensors, a design change is required to reduce cost while maintaining comparable precision.

The current design concept for CELT uses capacitor plates coated directly on the edges of the segments<sup>5</sup>. One segment has a single capacitor plate on its edge, while the segment across the inter-segment gap has two capacitor plates vertically spaced so as to overlap with this first plate, creating two capacitors. The sensor measures the differential capacitance between these two capacitors. This sensor is sensitive to the relative out-of-plane displacement of the two segments, since as the

segments move, one capacitor will increase in area while the other decreases. The response is a function of the gap size, hence the sensor is also sensitive to a change in the dihedral angle between the segments. A separate reading proportional to the sum of the two capacitors will be used to correct for the gain variation with changes in the gap. These edge sensors measure all of the internal modes of the segment array. We may also use a wavefront sensor to improve the precision of estimating low spatial frequency deformations of the array, as described in the next section.

No effort has been expended to date to investigate hardware for control computation; this is not expected to be a problem that will drive either technical feasibility or cost of the telescope.

## 5. Control Analysis

Contributions to the error budget from the active control system include actuator noise, sensor noise, uncontrolled frequencies (i.e. residual motion above the bandwidth of the control), and errors in the desired sensor readings. The first issue to address is whether a controller can be designed to meet the required optical precision given the current actuator and sensor specification. The second issue is bandwidth. This is more difficult to resolve in the absence of a structural model, but we consider whether it would be feasible to increase the control bandwidth beyond that used on Keck in order to compensate for wind-induced vibration. Finally, the computational requirements are briefly addressed at the end of this section.

### *Precision*

The error in the desired sensor readings results from the fact that zero on the sensor does not mean the segments are aligned unless the sensors are placed with tolerance of a few nm. The desired readings are determined with an alignment camera and are expected to contribute  $\theta(80)$  of 25 mas, or 8 nm wavefront error.

Each segment of the primary mirror has three out of plane degrees of freedom, and it is convenient to use the displacement at each of the actuator locations to describe the position of each segment. Thus the overall deformation of the primary mirror can be determined from the vector  $x$  of segment deflections at the actuator locations. The rms surface error of the primary mirror is  $S_{\text{rms}} = 1.06 \cdot \sigma_x$  (based purely on geometry), where  $\sigma_x$  is the rms of the vector  $x$ , and the rms wavefront error is double the rms surface error. The contribution to enclosed energy on the sky,  $\theta(80)$ , is obtained by ray-tracing analysis; for a Gaussian point spread function and uncorrelated displacement errors  $\sigma_x$ , the result is given by  $\theta(80) = 11.5 \cdot \sigma_x$  (this is specific to geometry

choices such as the distance between actuators and the center of a segment).

These relationships allow one to assess the impact of finite precision actuators. The total contribution to the error budget due to the 7 nm error allowed by the actuator requirement is 0.017 arcseconds (seeing limited) or 15 nm wavefront error (diffraction limited). This latter figure does not account for the fraction that is correctable with AO.

An initial analysis of the error propagation resulting from sensor noise is described in Ref. 6. With only the capacitive edge sensors, the low wave-number (spatially smooth) modes have poor observability, and thus the computed actuator moves amplify the sensor noise. Including wavefront information improves the observability of these low wave-number modes.

The vector of edge sensor readings  $y_e$  that result from segment displacements satisfies

$$y_e = A_e x + n,$$

where the matrix  $A_e$  is determined from the geometry, and  $n$  is the sensor noise. The singular value decomposition of  $A_e$  motivates a useful set of basis functions for representing spatial deflection shapes of the mirror. With  $A_e = U \Sigma V^T$ ,  $\Sigma$  a diagonal matrix of singular values  $\sigma_i$ , and  $U$ ,  $V$  unitary, then  $\xi = V^T x$  or  $x = V \xi$  is a useful change of basis; the columns of  $V$  will be referred to as “modes” for convenience, and represent a complete orthonormal set which span the space of all possible configurations of the primary mirror. Large singular values of  $A_e$  correspond to highly observable deflection shapes, which are those with large deflections between neighboring segments for unit overall rms deflection. Figure 6 gives a visualization of a typical high wave-number mode. Small singular values correspond to low spatial wavenumber deflection shapes, where there is relatively less deflection between segments for unit rms overall deflection; one of the first modes is shown in Figure 5. The matrix  $A_e$  has three singular values equal to zero, corresponding to overall rigid body deflection of the primary mirror. The focus mode (where every segment has the same dihedral angle between its neighbors) has zero relative edge displacement between segments, but is observable with the current sensor geometry.

The simplest control law is to estimate the deflections at the actuator locations as

$$\hat{x} = A^{\#} y,$$

and compute the desired change in the actuator commands  $u$  via

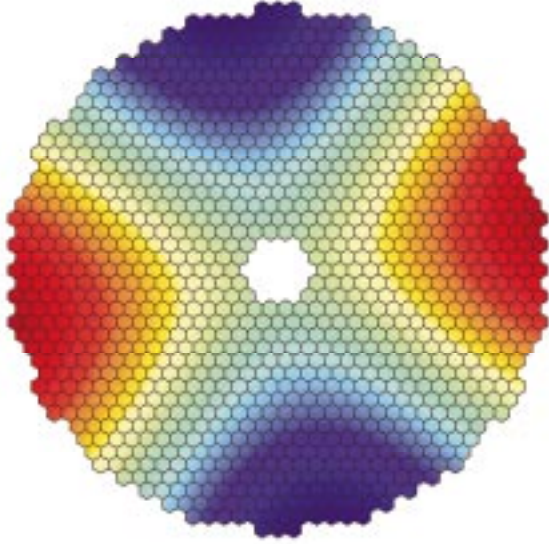


Figure 5. Mode 5, corresponding roughly to Zernike mode  $Z_{22}$ .

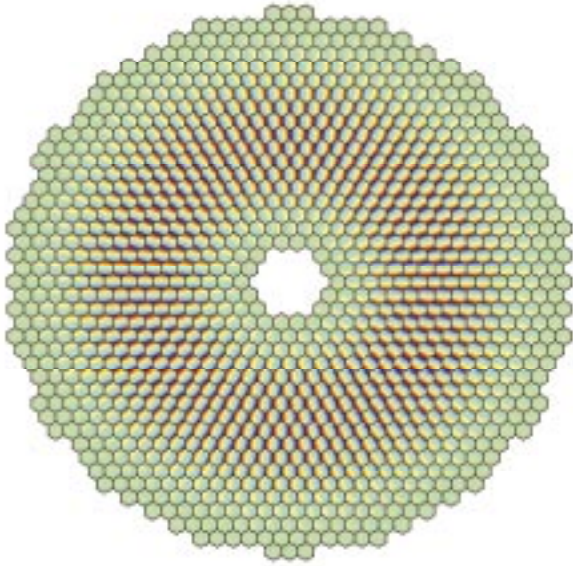


Figure 6. Most observable mode of  $A$  matrix, characterized by high inter-segment motion.

$$\Delta u = \beta \hat{x},$$

where  $A^\#$  is the left pseudo-inverse  $(A^T A)^{-1} A^T$  (readily computable from the singular value decomposition,  $A^\#$  has singular values  $\sigma_i^{-1}$ ) and  $\beta < 1$  determines the bandwidth. With this integral control law, deflections of any spatial shape are controlled with the same bandwidth. However, modes with small singular value in  $A$  have large singular values in  $A^\#$ , and hence the control law will amplify whatever sensor noise exists in these directions. Assuming white noise, then the overall noise propagation from rms sensor noise to rms

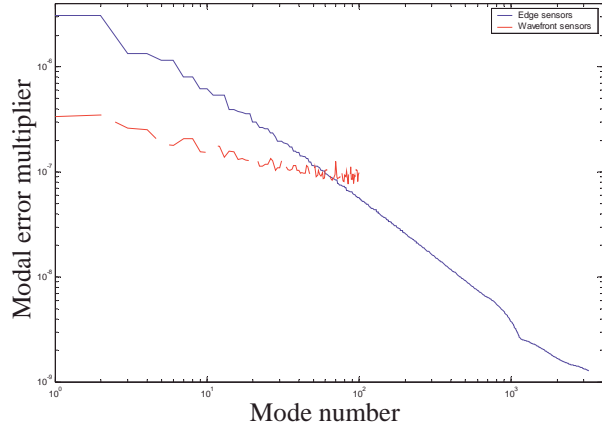


Figure 7. Scaled error multipliers for edge sensors (6 nm noise) and wavefront sensors (30 mas noise, dashed). Modes are numbered from lowest spatial wavenumber to highest. The error multiplier for the combined system will fall below both curves.

errors in estimating the deflection at the actuator locations is given by

$$\sigma_{x-\hat{x}} = (\sum \sigma^2(A)/n_a)^{1/2}$$

The resulting error in actuator positions depends on the control gain, and for  $\beta \ll 1$  is given by  $(\beta/2)^{1/2} \sigma_{x-\hat{x}}$ . The contribution to image blur is obtained by considering the rms segment rotation for each mode.

As noted earlier, the capacitive edge sensors described in Ref. 5 measure the differential capacitance between an upper and lower capacitor, and are sensitive to both vertical translation of neighboring segments, and to relative rotation about the axis defined by the segment edge. The first of these is much more significant, and at the time of writing Ref. 6, only the first was included. However, including the sensor response due to relative rotation between segments is significant because the “focus” mode becomes observable, and the low order modes also become slightly more observable. With the updated  $A$  matrix, the overall sensor noise amplification with only the edge sensors is estimated to be between 16 and 30, depending on the geometry assumed for the capacitive sensors. Regardless of sensor design, these estimates are significantly larger than the value of 4.4 for the 36-segment geometry of Keck. The redesigned sensors for CELT will be assumed to have the same 6 nm rms noise that is currently encountered at Keck. This yields an error of 95 nm rms in estimating the primary mirror deflection if only these sensors are used.

The displacement estimates for the low wave-number modes can be improved using optical wavefront information. A Shack-Hartmann wavefront sensor

measures the average wavefront tip and tilt on each element of an array of lenslets. The corresponding sensor influence matrix  $A_w$  is computed by averaging the tip/tilt errors of the segments that are mapped onto each lenslet. Since this information must be available anywhere in the sky, sufficient information must be obtainable from an 18.5 magnitude star. For a 90 lenslet array with realistic read noise, the sensor noise is roughly 30 mas. The edge and wavefront sensor information can then be combined to estimate the resulting error propagation. Figure 7 compares the modal error multipliers for the two different sensors, scaled by their respective noise levels, with modes ordered from lowest wave-number (least observable) to highest. The wavefront sensor provides better information for the first 50 modes. While the two sensors would ultimately be combined using a Kalman filter, for simplicity in our initial analysis we used the projection from the singular value decomposition of the edge sensor  $A$  matrix, and applied only wavefront information for the first 50 modes, and only edge sensor information for the remaining modes. This gives a 6-fold reduction in the overall sensor noise error relative to using edge sensor information only, yielding 14 nm rms surface, or 28 nm wavefront estimation error.

With the same bandwidth as Keck ( $\beta = 0.1$ , bandwidth  $\sim 0.03$  Hz), the final wavefront error is roughly 6 nm. A bandwidth of 0.1 or 1 Hz would result in sensor noise contribution of 11 or 35 nm rms wavefront error respectively. Even with the wavefront sensing, the control errors resulting from this sensor noise are primarily in low wave-number modes. Since these modes can easily be controlled by the adaptive optics system, the sensor noise contribution to the error budget is not an issue with AO on<sup>5</sup>. For seeing-limited observations, the combined wavefront / edge sensor noise propagation results in  $\theta(80)$  for 0.03, 0.1, or 1 Hz bandwidths of 2, 3, and 9 mas respectively.

Combining the precision estimates from the four sources (15 nm wind, 8 nm error in desired sensor reading, 15 nm actuator precision and 6 nm sensor noise) yields roughly 23 nm contribution to the primary mirror wavefront error with AO on, which is within the desired error budget. Similarly for seeing-limited observations the desired specification can be met. It should be emphasized that the estimates presented are dependent on many assumptions, however this preliminary conclusion is promising.

#### *Bandwidth*

The desired bandwidth of the primary mirror control depends on the wind disturbance model. At Keck, the primary mirror control has an extremely low bandwidth sufficient to compensate for gravity and thermal

deformations, but not for wind loading. It is possible that higher control bandwidths may need to be considered for CELT. The pressure spectra measured at Gemini have corner frequencies of  $\sim 0.1 - 0.3$  Hz, and typically less than 10% of the wind energy is above 1 Hz. Thus a bandwidth of 1 Hz would cut the wind-induced rms vibration by 2/3.

The achievable bandwidth is likely to be limited by interaction with structural modes. The resonance of a segment on its support for Keck is roughly 30 Hz, and this of course varies slightly between segments, and varies with orientation of the telescope. The overall structural model for Keck, including both segment dynamics and the mirror cell, has resonances as low as 10 Hz, and the interaction with these mirror cell modes limited the achievable bandwidth at Keck to about 0.5 Hz or less to avoid instability<sup>11</sup>. Because of the difficulty of adding passive damping at the low vibration levels encountered, many of the modes on Keck have an estimated quality factor  $Q \approx 100$ . Notch filtering at the resonance frequency cannot be used because of the number of resonances, the exact frequencies of which are unknown. A slight increase in bandwidth might be obtained by increasing the order of the controller. However, achieving a bandwidth sufficient to control a useful fraction of wind-induced vibration will probably require some passive damping of the mirror cell and the segment support resonances. The lowest CELT mirror cell modes are estimated to be half the frequency of the equivalent Keck modes, hence achieving a 1 Hz bandwidth would require passive damping to reduce  $Q$  to roughly 25.

As discussed in the previous subsection, increasing the control bandwidth will increase the noise amplification, and without better sensors, a 1 Hz bandwidth is unacceptable. However, higher bandwidth can be used on the higher wave-number modes that are influenced by wind vibration, while the bandwidth on lower wave-number modes is kept small to avoid sensor noise.

#### *Computation*

An additional control characteristic that needs to be estimated is the computational cost of the control law, as this could impact achievable bandwidth, or require additional design effort. The sample rate is likely to be no more than 10 Hz, which would be marginally adequate to achieve a worst-case bandwidth of 1 Hz. Thus, in the worst case, executing the control requires the multiplication of a fully populated 3240 by 6386 matrix with the vector of sensor readings (including both 6204 edge sensors and a 91 element wavefront sensor giving two components of information per element) at a 10 Hz rate or roughly  $2 \times 10^8$  flops. This does not include error checking on sensor information,

nor the time required to move information within the computer. However, these computations are not unreasonable for currently available hardware.

If the computations are problematic, a simple solution is to not use every single edge sensor in computing the response of each actuator. That is, replace the exact (global) control law with an approximate (local) one in which one considers only the effect of sensors in a neighborhood of a given actuator to determine the appropriate actuator command. The fully-populated matrix inverse  $A^\#$  uses all of the sensor information primarily for the low wave-number modes. If many of these degrees of freedom are estimated with wavefront information, then convergence is still adequate while restricting information connectivity to only the segment of interest and some neighboring segments. A hierarchic approach could also be used to estimate the first set of modes globally. In either case, rather than using all 6386 pieces of information to determine each actuator command, several hundred would likely suffice, dropping computation by more than an order of magnitude. Similar approaches have been analyzed in Ref. 18. While none of these approaches has been fully analyzed for CELT, computation is not considered to be a problem at this time.

## 6. Additional Control Issues

The primary mirror is not the only part of CELT that will require control. The secondary mirror will deflect roughly 1 to 1.5 cm under gravity, and thus will require low bandwidth actuation to compensate for this motion. Wind deflections may necessitate five degree of freedom control on the secondary, with a bandwidth of  $\sim 1$  Hz. The control of the secondary mirror has not yet been considered in detail, since with only a few degrees of freedom, the system will not be a significant element of the overall telescope cost, nor does it appear likely to be a barrier to feasibility.

Adaptive optics will also be an essential part of the CELT design; to enable diffraction limited images at wavelengths as short as  $1\mu\text{m}$  requires controlling as many as 7000 modes of the atmosphere, at several different layers. The resulting AO system may have multiple deformable mirrors and wavefront sensors totaling tens of thousands of degrees of freedom<sup>19</sup>. While the primary mirror control is intended to keep the primary mirror in the correct shape, and the adaptive optics intended to compensate for atmospheric distortion, the two systems act as an integrated system to provide the correct wavefront to the instrumentation, regardless of the source of the distortion. While segment edge discontinuities produce wavefront errors impossible to correct using the deformable mirrors, low wavenumber primary mirror deformation can be

corrected by the AO. Subject to bandwidth and stroke limitations, four scenarios can be considered: (i) independent design of active and adaptive optics, (ii) primary mirror control offloading low-bandwidth, high stroke requirements from the AO system, (iii) AO system correcting spatially smooth, moderate bandwidth (e.g. wind-induced) vibration that is above the primary mirror control bandwidth, or (iv) complete coupling between AO and primary mirror control.

## 7. Summary and Conclusions

The California Extremely Large Telescope presents some challenging control problems. The current design concept uses over 3000 actuators and over 6000 sensors. Cost is therefore a significant issue driving feasibility. The initial concept design phase includes goals to be completed by the end of 2001 to (i) estimate disturbances, (ii) select, prototype, and test a nominal actuator and sensor design, and (iii) complete the error budgets. Based on these we will make cost estimates for actuators and sensors and identify remaining issues.

Preliminary analysis, however, leads us to conclude that the control problem is likely to be feasible, relative to both technical and cost goals. Several actuator approaches have been identified that will enable significant unit cost reductions relative to the Keck telescope, while achieving the stroke, resolution, and lifetime goals of CELT. Wind disturbances may impact the primary mirror, but it may be possible to increase the control bandwidth sufficiently to compensate.

Issues that are currently being addressed or will be addressed include:

- Refining several actuator concepts in order to validate the ability to meet technical specifications, cost, and reliability.
- Improving the estimate of the sensor noise level achievable with the capacitive edge sensors.
- Completing the wavefront sensor design.
- Determining the best combination of wavefront and edge sensors, and finalizing the resulting contribution to the error budget.
- Investigating algorithms to reduce control computation.
- Improving estimates of wind-induced vibration on the primary, including the reduction in wind speed, and the spatial correlation over the mirror.
- Completing initial structural design and analysis to determine resonant frequencies and mode shapes of the mirror cell structure, and thus assess the achievable control bandwidth.
- Assessing the potential for damping the structure.
- Developing actuators for position control of the secondary mirror.

## Acknowledgements

The work discussed here benefited from numerous discussions with other members of the CELT team. Alan Schier of the Pilot Consulting Group conducted a study of actuator options.

## References

- <sup>1</sup> Nelson, J.E. "Design Concepts for the California Extremely Large Telescope (CELT)", SPIE **4004**, 2000.
- <sup>2</sup> Nelson, J and Mast, T., "Giant Optical Devices", *Proceedings, Backaskog Workshop of Extremely Large Telescopes*, June 1999.
- <sup>3</sup> Jared, R.C. *et al.* "The W.M. Keck Telescope segmented primary mirror active control system," SPIE **1236 Advanced Technology Optical Telescopes IV**, pp. 996-1008, 1990.
- <sup>4</sup> Cohen, R., Mast, T., and Nelson, J., "Performance of the W.M. Keck Telescope Active Mirror Control System," SPIE **2199**, pp. 105-116, 1994.
- <sup>5</sup> Mast, T. and Nelson, J. "Segmented Mirror Control System Hardware for CELT", SPIE **4003**, 2000.
- <sup>6</sup> Chanan, G., Nelson, J., Ohara, C., and Sirko, E. "Design Issues for the Active Control System of the California Extremely Large Telescope (CELT)", SPIE **4004**, 2000.
- <sup>7</sup> Smith, D.R., "Wind Tests Data from Gemini South May 13-14 2000" (on CD) *Aura New Initiatives Office*, 2001.
- <sup>8</sup> Kiceniuk, T., and Potter, K., "Internal air flow patterns for the Keck 10 meter telescope observatory dome", Keck observatory report #166, or GALCIT 10' GWT – DR 1104, April 1986.
- <sup>9</sup> DeYoung, D., "Numerical Simulations of Airflow in Telescope Enclosures", *The Astronomical Journal*, **112**(6): 2896-2908, 1996.
- <sup>10</sup> Budiansky, M. and Nelson, J., "TMT Site Wind Characteristics", Keck Observatory Report #130, 1985.
- <sup>11</sup> Aubrun, J.-N., Lorell, K.R., Mast, T.S., and Nelson, J.E., "Dynamic Analysis of the Actively Controlled Segmented Mirror of the W.M. Keck Ten-Meter Telescope," *IEEE Control Systems Magazine*, pp. 3-10, Dec. 1987.
- <sup>12</sup> Meng, J.D. *et al.*, "Position actuators for the primary mirror of the W.M. Keck telescope," SPIE **1236**, 1990.
- <sup>13</sup> Schier, A., "Summary of the CELT Mirror Segment Actuator Survey", CELT Report #15, (available at <http://celt.ucolick.org>), Feb. 2001.
- <sup>14</sup> Chen, Q., Yao, D.-J., Kim, C.-J., and Carman, G., "Development of Mesoscale Actuator Device with Micro Interlocking Mechanism", *J. Intelligent Material Systems and Structures*, vol 9, pp. 449-457, June 1998.
- <sup>15</sup> Chen, Q., Yao, D.-J., Kim, and Carman, G.P., "Mesoscale actuator device: Micro interlocking mechanism to transfer macro load", *Sensors and Actuators*, Vol. 73, pp. 30-36, 1999.

- <sup>16</sup> Prechtel, E.F., and Hall, S.R., "Design of a high-efficiency discrete servo-flap actuator for helicopter rotor control", *SPIE Smart Structures and Materials conference*, 1997, pp 158-182. SPIE paper # 3041-15.
- <sup>17</sup> Minor, R.H., Arthur, A.A, Gabor, G. and Jackson, H.G., "Displacement sensors for the primary mirror of the W.M. Keck telescope," SPIE **1236**, 1990.
- <sup>18</sup> Li, K., Kosmatopoulos, E.B., Ioannou, P.A., and Ryaciotaki-Boussalis, H., "Large Segmented Telescopes: Centralized, Decentralized, and Overlapping Control Designs", *IEEE Control Systems Magazine*, pp. 59-72, October 2000.
- <sup>19</sup> Dekany, R., Nelson, J.E., and Bauman, B., "Design considerations for CELT adaptive optics", SPIE **4003**, 2000.